Seismic Wave Propagation in a Multi-Layered Geological Region, Part I*: Non-Elastic Steady State Case

Petia Dineva[1] and Elena Gavrilova[2]

1. Institute of Mechanics, Bulgarian Academy of Science, Sofia, Bulgaria, email: Petia@imbm.bas.bg

2. Department of Mathematics, University of Mining & Geology, St. Ivan Rislski, Sofia, Bulgaria, email: Elenag@iterra.net

ABSTRACT: *The Direct Boundary Integral Equation Method (DBIEM) studies the two-dimensional "in-plane" steady-state wave propagation problem in a non-elastic multi-layered region with non-parallel boundaries. Wave attenuation and dispersion due to the non-elastic soil behavior are investigated by the generalized Maxwell-Gurevich model (GMG model). The numerical example solved considers two real geological situations for a multi-layered soil media with existence of salt ore deposits. These situations concern one and the same geological region but in different periods of its exploitation in 1951 and 1994. There is a change of the situation during the years when the exploitation of the salt ore deposits has been done. The region is subjected to incident time-harmonic seismic P-waves. Theoretical amplitude-frequency characteristics at the free-surface points for elastic and non-elastic cases are obtained and compared.*

Keywords: Wave attenuation and dispersion by the GMG-model; Multi-layered geological region; DBIEM; Steady state wave problem

1. Introduction

On the basis of the review of the experimental results one can see that there are two different kinds of seismic waves dispersion. One kind of dispersion is due to the non-elastic soil behavior and in this case the damping coefficient $\alpha \left[m^{-1} \right]$ depends linearly on the frequency. Then the wavelength $\lambda > 10 - 20D$, where D is the inhomogeneity size. The other kind of dispersion is due to the wave geometrical scattering and it occurs at $\lambda \geq D$ and $\alpha(\omega) \sim \omega^2$, where ω is the frequency. The experimental dispersive curve $\alpha(\omega)$ is a line-due to the energy damping at microstructure state change and non-elastic deformation, with some fluctuations on it due to the scattering from inhomogeneities in soil [1]. Figures (1a) and (1b) show the experimental dispersive curves $\alpha(\omega)$, obtained in [1] for soil materials. The basic dispersion relations: velocity $V(\omega)$ and attenuation coefficient $\alpha(\omega)$, obtained from classical models of Foight, Maxwell and linear standard body model, do not agree with the experiment in a vast zone of frequencies. Except for the classical models, many authors give their contribution to the creation of physical models of soil. Well-known are the models of Deriagin [2], Lomnitz [3], Futerman [4], Knopoff [5], Isacovich [6], Magnitski and Jarkov [7], Biot and

Frankel [8, 9]. None of them, however, shows satisfactory agreement with the experimental results.

The main aims of this paper are:

❖ To present the essence of the GMG model for describing the physical dispersion of the seismic waves and its use in modeling of two-dimensional "in-plane" wave propagation in a multi-layered non-elastic geological region with complex geometry. The motivation for this is that this model gives theoretical results for attenuation and dispersion of seismic waves in soil, which are in good agreement with the experimental data [10].

❖ To show that the changes in the soil region during the years of the exploitation process lead to the change in its dynamic response, i.e. to the change in the obtained theoretical amplitude-frequency characteristics.

The paper is organized as follows: The description of the GMG model is presented in section 2 and the two-dimensional wave equation using the GMG model is discussed in section 3. The formulation of the problem is given in section 4. Section 5 presents BIEM formulation of the considered problem. Some numerical results are given in section 6. The conclusion is made in section 7.

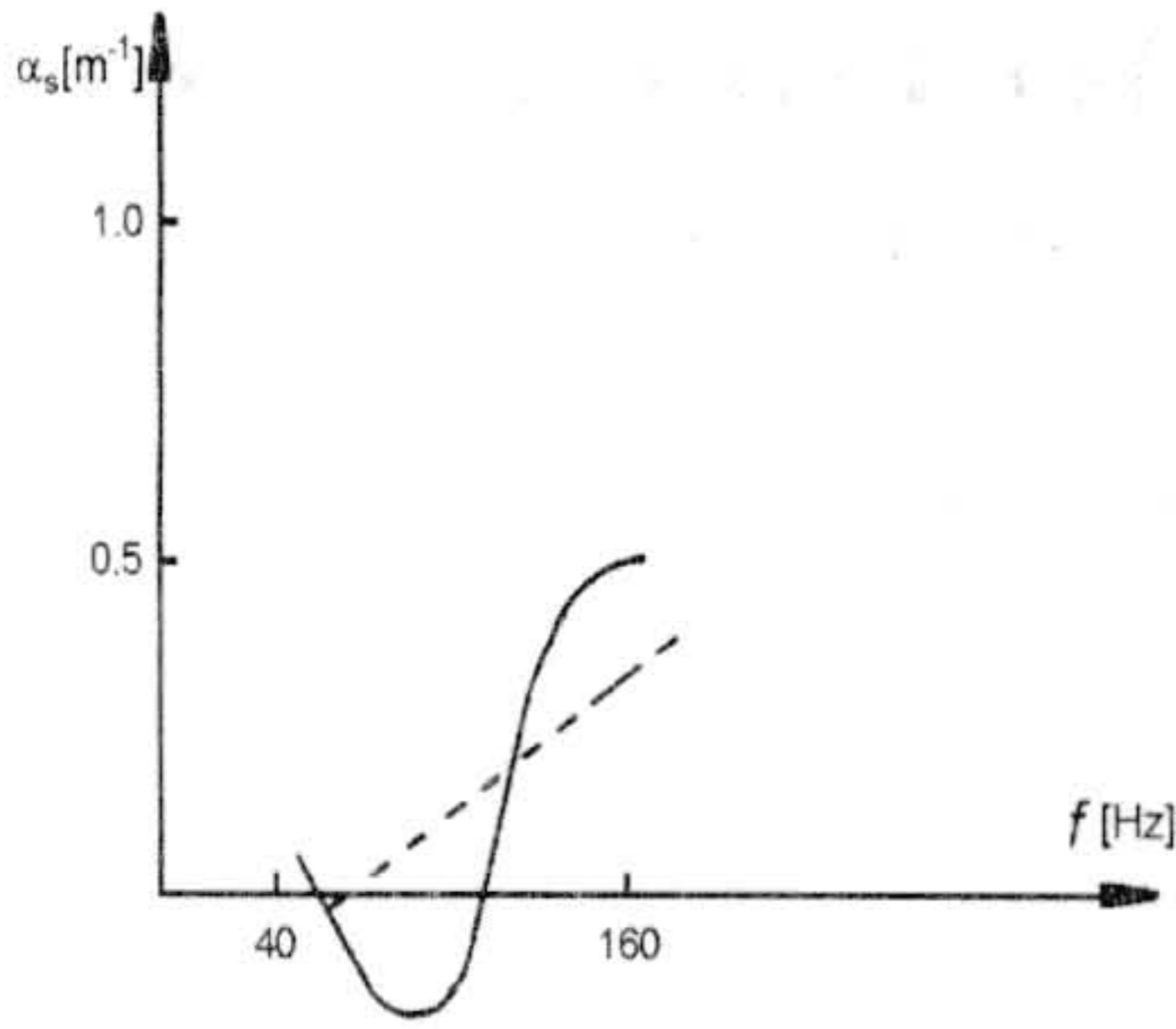** Part two of this paper will be published in the next issue of JSEE.*

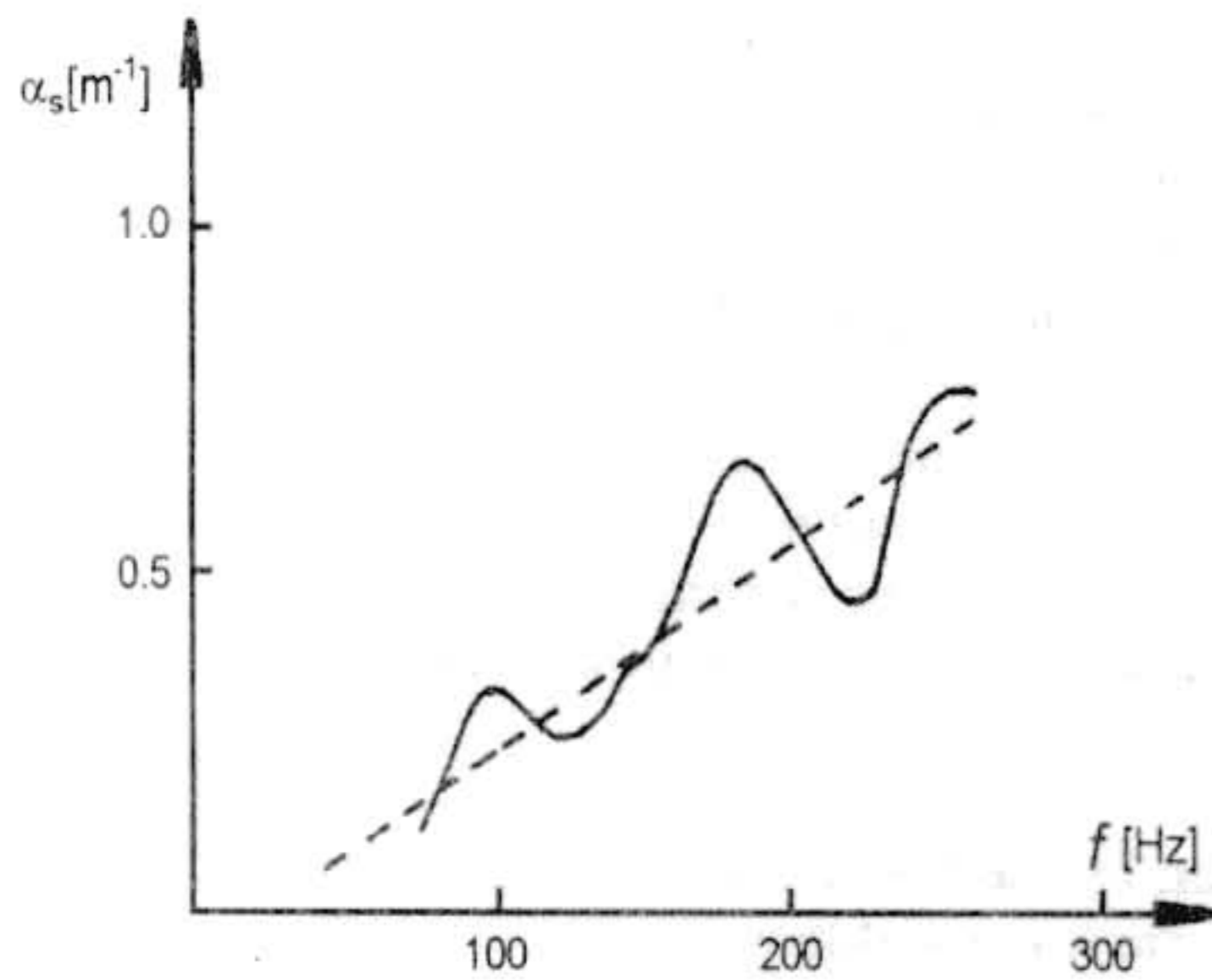Figure 1a. Experimental dispersive curve $\alpha(f), f = \dfrac{\omega}{2\pi}$.

Figure 1b. Experimental dispersive curve $\alpha(f), f = \dfrac{\omega}{2\pi}$.

2. Description of the GMG Model

In the seventies, Gurevich [10] reached to the viewpoint of Maxwell for solid deformation mechanism in the case of wave propagation far from the wave source (in the case of small deformation $\varepsilon_{ij} : 10^{-4} - 10^{-6}$). The total deformation ε_{ij} is a sum of the elastic deformation ε_{ij}^{e} and the linear elasto-relaxational deformation ε_{pij} that develops and damps in time

$$\varepsilon_{ij} = \varepsilon_{ij}^{e} + \varepsilon_{pij} \tag{1}$$

Gurevich [10] adopts Maxwell's molecular idea about the character of the elasto-relaxational deformation, see Figure (2). Under acoustic load the total deformation is
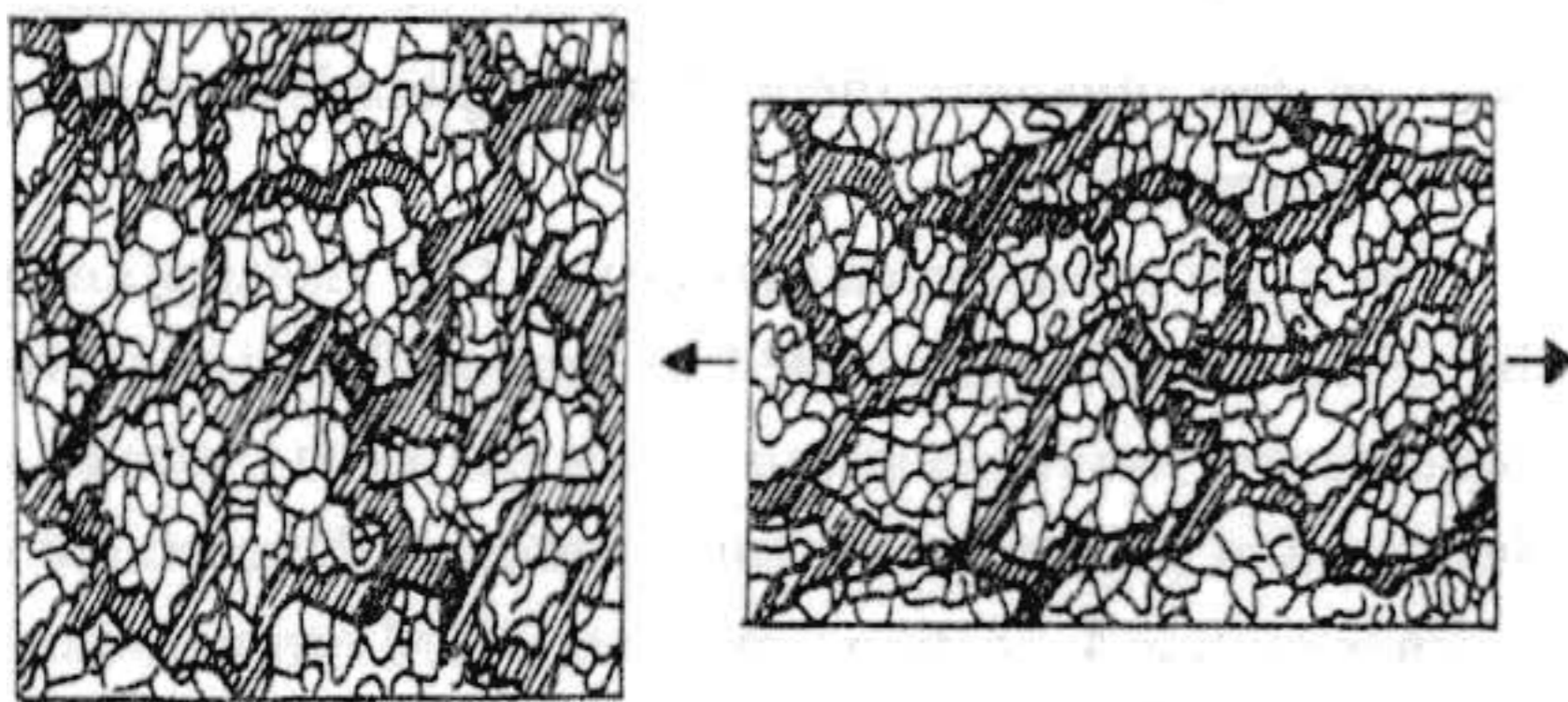

Figure 2. Gurevich's viewpoint for solid deformation in soil.

$\varepsilon_{ij} << 1$ and the weakest molecular bonds are destroyed. Molecules strongly bonded surround the micro-particles, between which the bound have been destroyed, and these molecules form an elastic skeleton of the body. There, phases of stresses and strains coincide and Hook's law links stress and strain. Due to the destruction of the weak bonds in the skeleton from time to time, and to corresponding reorganization of the skeleton molecules, there occurs elasto-relaxational strain ε_{pij}, which does not coincide with the stress phase. The irreversible deformation does not exist. This model is valid for waves with small amplitude for isothermal process, macroscopic homogeneous and isotropic medium. The first members of the Taylor's series of the function $\sigma_{pij} = f(\varepsilon_{pij})$ are considered, i.e. the elasto-relaxational deformation takes place

$$\sigma_{pij} = \lambda_p^* \Theta_p \delta_{ij} + 2\mu_p^* \varepsilon_{pij}, \Theta_p = \sum_i \varepsilon_{pii}, i,j = x,y \tag{2}$$

Here λ_p^* and μ_p^* are structure parameters, characterizing the elasto-relaxational properties which are called Lame relaxational coefficients. The value of the relaxational stress σ_{pij} is determined by a traction σ_{ij}, such as $\varepsilon_{pij} = 0$, i.e. this traction stops the elasto-relaxational deformation at a given moment of time t^*, when

$$\sigma_{ij} = \sigma_{pij} \tag{3}$$

Then the following relations can be written

$$\varepsilon_{ij} = \varepsilon_{ij}^{*e} + \varepsilon_{pij}^{*}, \quad \mu\left(\varepsilon_{ij}^{*e} - \frac{\delta_{ij}\Theta^{*e}}{3}\right) = \mu_p^*\left(\varepsilon_{pij}^{*} - \frac{\delta_{ij}\Theta_p^{*}}{3}\right)$$

$$\Theta = \Theta^{*e} + \Theta_p^{*}, \quad K\Theta^{*e} = K_p^* \Theta_p^{*} \tag{4}$$

$$\Theta^{*e} = \sum_{i=1}^{3} \varepsilon_{ij}^{*e}$$

Here K and K_p^* are the elastic and relaxational volume module; μ and μ_p^* are the elastic and relaxational shear module; δ_{ij} - the Kronecker delta; ε_{ij}, Θ - the total deformation; $\varepsilon_{ij}^{*e}, \Theta^{*e}, \varepsilon_{pij}^{*}, \Theta_p^{*}$ -the elastic and relaxational strains at a moment of time t^*, when $\sigma_{ij} = \sigma_{pij}$ and $\varepsilon_{pij} = 0$. In fact, the condition $\sigma_{ij} = \sigma_{pij}$ is a stability condition. The difference between materials lies in the path they take to arrive at the final stability state. This depends on the behavior of the concrete microstructure, i.e. on the structural module- $K, K_p^*, \mu, \mu_p^*, \rho, T_P, T_M$. Here T_P is the time for transition from some equilibrium state into another one for one molecule; T_M is the time for transition of a group of molecules from some state of equilibrium into another one; and ρ is density. The quantities $\varepsilon_{ij}^{e}, \Theta^{e}, \varepsilon_{pij}, \Theta_p$ become $\varepsilon_{ij}^{*e}, \Theta^{*e}, \varepsilon_{pij}^{*}, \Theta_p^{*}$ by instantaneous transition act to a stable structure in the case when the total deformation does not change at this time, so that the strong bonds in the elastic skeleton are conserved. At each other moment $t \neq t^*$, when the condition $\varepsilon_{pij} = 0$ is

not fulfilled

$$\varepsilon_{ij} = \varepsilon_{pij}^{e} + \varepsilon_{pij} \text{ and } \Theta = \Theta^{e} + \Theta_{p} \tag{5}$$

Gurevich gives a definition of elasto-relaxational strain rate as

$$\dot{\varepsilon}_{pij}\left(T_{P}^{*}\right) = \frac{\varepsilon_{ij}^{e} - \varepsilon_{ij}^{*e}}{T_{P}^{*}} \tag{6}$$

Using Eqs. (4, 5 and 6), it is obtained in [10]

$$\frac{\partial \Theta_{p}\left(T_{p}^{*}\right)}{\partial t} = \left[\frac{\Theta^{e}}{K_{p}^{*}} - \frac{\Theta_{p}\left(T_{p}^{*}\right)}{K}\right]\frac{G}{T_{p}^{*}} \tag{7}$$

$$\frac{\partial}{\partial t}\left[\varepsilon_{pij}\left(T_{p}^{*}\right) - \frac{\delta_{ij}\Theta_{p}\left(T_{p}^{*}\right)}{3}\right] =$$

$$\frac{g}{T_{p}^{*}}\left[\frac{\varepsilon_{ij}^{e} - \frac{\delta_{ij}\Theta^{e}}{3}}{\mu_{p}^{*}} - \frac{\varepsilon_{pij}\left(T_{p}^{*}\right) - \frac{\delta_{ij}\Theta_{p}\left(T_{p}^{*}\right)}{3}}{\mu}\right]$$

where $g = \dfrac{\mu\mu_{p}^{*}}{\mu + \mu_{p}^{*}}$, $G = \dfrac{KK_{p}^{*}}{K + K_{p}^{*}}$ and T_{p}^{*} is a relaxation time- it is the time necessary for a group of molecules to pass from a given equilibrium state to another one. Gurevich generalized Maxwell's "time of relaxation". According to him, it depends on the material structure properties, microstructure state, temperature and traction applied to the body

$$T_{p}^{*} = c\tau_{0}exp\left(\frac{U^{*}}{k_{B}\Theta_{t}}\frac{\tilde{v}}{\tilde{v}_{a}}\right) \tag{8}$$

Here c is a structural constant, depending on the microstructure state properties; τ_{0} is the time for particle jump of some equilibrium state to another; k_{B} - Boltzman's constant; Θ_{t} - the absolute temperature; U^{*} - the activation energy, necessary for overcoming of the potential barrier at transition from some state to another; $\tilde{v} \in [\tilde{v}_{a}, \tilde{v}_{max}]$, where $\tilde{v}_{a}$ is the volume of one molecule and $\tilde{v}_{max}$ is the maximum volume of molecule group that jumps from some state to another. The Gurevich's point of view is that T_{p}^{*} is a function of σ_{ij} and Eq. (7) is non-linear. However, Gurevich has not determined the relation $T_{p}^{*}(\sigma_{ij})$, which demands accounting for the microstructure state change. As a result, his model at this stage is a linear physical equation. Gurevich assumes that not only one relaxational time occurs in a solid, but that there exists a spectrum of relaxational times

$$\frac{\partial \varepsilon_{pij}}{\partial t} = \int_{T_{P}}^{T_{M}} \frac{\partial \varepsilon_{pij}\left(T_{P}^{*}\right)}{\partial t} \frac{dT_{P}^{*}}{T_{P}^{*}} \tag{9}$$

The GMG constitutive equation is obtained in [10] using Eqs. (7) and (9)

$$\varepsilon_{ij} = \varepsilon_{ij}^{e} + \varepsilon_{pij}, \dot{\sigma}_{jj} = \mu\left(2\frac{\partial \dot{u}_{j}}{\partial x_{j}} + \frac{2v}{1-2v}\dot{\Theta} - \dot{\varepsilon}_{pjj}\right)$$

$$\dot{\sigma}_{jk} = \mu\left(\frac{\partial \dot{u}_{k}}{\partial x_{j}} + \frac{\partial \dot{u}_{j}}{\partial x_{k}} - \dot{\varepsilon}_{pjk}\right) \tag{10}$$

where v is Poisson coefficient

$$R = ln\frac{T_{M}}{T_{P}}; \ \xi = \frac{T_{M}}{T_{P}^{*}}; \ \mu_{p} = \frac{\mu_{P}^{*}}{R}; \ K_{P} = \frac{K_{P}^{*}}{R} \tag{11}$$

$$\dot{\varepsilon}_{pij} = \frac{1}{T_{P}R}\frac{g}{\mu_{p}}\int_{e^{-R}}^{1}e^{-\frac{gt}{\mu Tp}\xi}\int_{0}^{t}e^{-\frac{gt}{\mu Tp}\xi}\dot{\sigma}_{ij}dtd\xi$$

$$\dot{\varepsilon}_{pii} = \frac{1}{T_{P}R}\frac{g}{\mu_{p}}K + \frac{1}{T_{P}R}\frac{g}{\mu_{p}}L$$

$$K = \int_{e^{-R}}^{1}e^{-\frac{gt}{\mu Tp}}d\xi\left[\int_{0}^{t}e^{-\frac{gt}{\mu Tp}\xi}\left(\dot{\sigma}_{ii} - \sum_{i}\dot{\sigma}_{ii}\right)dt + D_{ii}(\xi)\right]d\xi$$

$$L = \int_{e^{-R}}^{1}e^{-\frac{gt}{\mu Tp}}d\xi\left[G(K_{p})^{-1}e^{\frac{GT}{KTp}\xi}\int_{0}^{t}e^{\frac{GT}{KTp}}d\xi \times\right.$$

$$\left.\left(\sum_{i}\dot{\sigma}_{ii}\right)dt + D(\xi)\right]d\xi$$

$$D_{ii}(\xi) = \left\{\varepsilon_{ii}^{e} - \frac{\Theta^{e}}{3} - \frac{\mu_{p}R}{\mu}\left[\varepsilon_{pii}\left(T_{P}^{*}\right) - \Theta_{P}\left(T_{P}^{*}\right)/3\right]\right\}_{t=t_{0}}$$

$$D(\xi) = \left\{\Theta^{e} - \frac{K_{p}R}{K}\Theta_{P}\left(T_{P}^{*}\right)\right\}_{t=t_{0}}$$

The above Eqs. (10) and (11) present the generalized Maxwell-Gurevich model obtained by Gurevich in [10] as a result of his concept for the molecular nature of the deformation process. The main advantage of this model is that it gives a possibility for connection between the soil microstructure characteristics and its stress-strain macro-behaviour. The procedure for the determination of the GMG model material constants is given in [10].

3. Two-Dimensional Wave Equation Using the GMG Model

After substituting of the constitutive Eqs. (10, 11) in the equation of motion

$$\sigma_{ij,i} = \rho\ddot{u}_{j} \tag{12}$$

the wave equation for a solid described by the GMG model is obtained. In case of two-dimensional plane-strain state the next wave equation is valid

$$\frac{\partial}{\partial t}\left\{\frac{\partial^2 u_i}{\partial t^2} - \frac{1}{\rho}\left[(\lambda+\mu)\frac{\partial\theta}{\partial x_i} + \mu\Delta u_i\right]\right\} +$$

$$\frac{\mu}{\mu_p R}\int\limits_{S_m}^{S_M}\left\{e^{-st}\int\limits_0^t e^{st}\frac{\partial}{\partial t}\left[\frac{\partial^2 u_i}{\partial t^2} - \frac{K}{\rho}\frac{\partial\theta_x}{\partial x_i}\right]dt\right\}ds +$$

$$\frac{K}{K_p R}\int\limits_{S_{m'}}^{S_{M'}}\left\{e^{-st}\int\limits_0^t e^{st}\frac{\partial}{\partial t}\left[\frac{K}{\rho}\frac{\partial\theta_x}{\partial x_i}\right]dt\right\}ds = 0$$

$$i = x, y \tag{13}$$

where

$$\theta = \varepsilon_{xx} + \varepsilon_{yy} = \frac{\partial u_x}{\partial x} + \frac{\partial u_y}{\partial y};\ \Delta u_x = \frac{\partial^2 u_x}{\partial x^2} + \frac{\partial^2 u_x}{\partial y^2}$$

$$\Delta u_y = \frac{\partial^2 u_y}{\partial x^2} + \frac{\partial^2 u_y}{\partial y^2};\ S = \frac{g\xi}{\mu T_P}$$

$$S_M = \left\{\left[1 + \frac{\mu}{\mu_p R}\right]T_P\right\}^{-1};\ S_m = \left\{\left[1 + \frac{\mu}{\mu_p R}\right]T_M\right\}^{-1}$$

$$S_{M'} = \left\{\left[1 + \frac{K}{K_p R}\right]T_P\right\}^{-1};\ S_{m'} = \left\{\left[1 + \frac{K}{K_p R}\right]T_M\right\}^{-1}$$

The authors' aim is to obtain the Helmholtz equation analogue of the two-dimensional GMG wave Eq. (13) in the case of time-harmonic seismic waves. We look for the solution of Eq. (13) in the form

$$u_i = u_{i0}e^{-i\omega t} \tag{14}$$

Here ω is the frequency, $u_{i0}(x, y)$ is the wave amplitude. Through substituting Eq. (14) in Eq. (13) and after some transformations, the Helmholtz equation, analogous in the case of the GMG model for soil, is obtained

$$\left[\left(\frac{k_s^*}{k_p^*}\right)^2 - 1\right]\left(\frac{\partial^2 u_{x0}}{\partial x^2} + \frac{\partial^2 u_{y0}}{\partial x \partial y}\right) + \left(\frac{\partial^2 u_{x0}}{\partial x^2} + \frac{\partial^2 u_{x0}}{\partial y^2}\right) =$$

$$- (k_s^*)^2 u_{0,x}$$

$$\left[\left(\frac{k_s^*}{k_p^*}\right)^2 - 1\right]\left(\frac{\partial^2 u_{y0}}{\partial y^2} + \frac{\partial^2 u_{x0}}{\partial x \partial y}\right) + \left(\frac{\partial^2 u_{y0}}{\partial x^2} + \frac{\partial^2 u_{y0}}{\partial y^2}\right) =$$

$$- (k_s^*)^2 u_{0,y} \tag{15}$$

The complex wave vectors k_s^* and k_p^* depend on the physical module of the GMG model

$$k_i^* = k_i + i\alpha_i;\ k_i = \frac{\omega}{V_i};\ i = s\text{ or }p \tag{16}$$

Here $\alpha_{s,p}$ is the wave-damping coefficient; $V_{s,p}$ - the shear or the longitudinal wave velocity. The shear and longitudinal wave vectors as well as the damping coefficients depend on the GMG model parameters.

The GMG model shows the linear dependence $\alpha(\omega)$ and weak dispersion dependence $V_S(\omega)$ as it is at the experimental results, see Figure (3). It is shown by the results in [10], that the GMG model gives a good agreement with the experimental results for different types of the soil material.
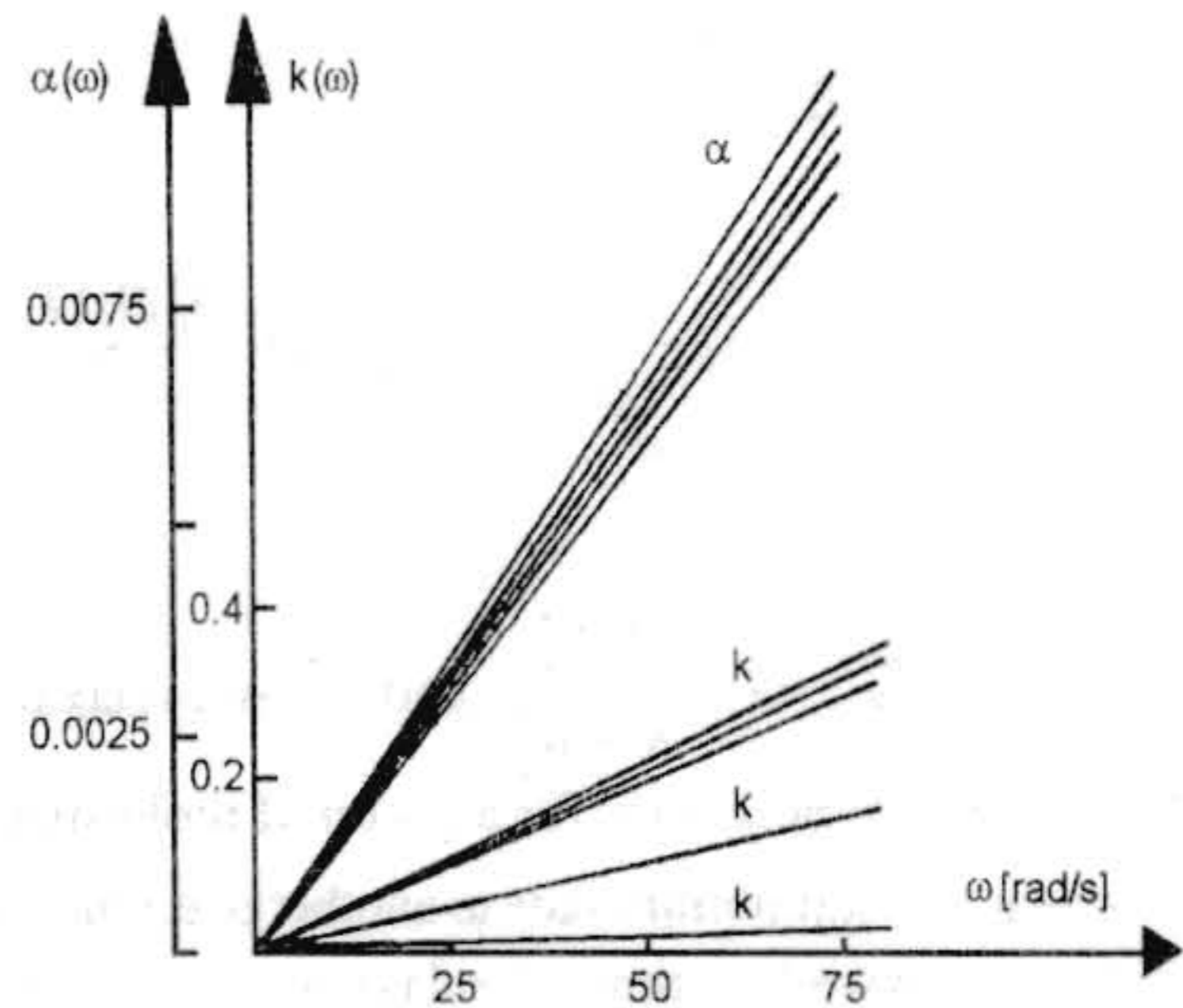

Figure 3. Dispersion curves $\alpha(\omega)$ and $k(\omega)$ obtained by the GMG model.

4. Formulation of the Problem

The nature of the ground motion during earthquakes can be significantly affected by the local site effects, such as layers. These local conditions can generate large amplifications and important spatial variations of the ground shaking. The generalized scattered motion determines the seismic load of structures in the geological region. The spatial variation of this ground motion is important for the analysis of structures with large dimensions such as bridges and dams, for assessing seismic risk, and for seismic design of important facilities.

The aim of this item is to formulate the steady state seismic wave propagation problem in a non-elastic soil multi-layered region using both the generalized GMG model to describe the non-elastic soil behavior and BIEM as a tool for solution of such a complex boundary-value problem.

The propagation of elastic waves through layered half-space is of considerable interest to engineers, geologists and seismologists. Lacking any analytical method to treat such problems, resort has been made to the numerical techniques-FEM and BIEM. The first systematic approach to multi-layered media may be traced

back to Thompson [13]- Haskell [14] methods, Gilbert and Baskus [15] introduced the propagator matrix method, Fuchs [16] introduced the reflectivity method, Pao and Gajewski [17] proposed the generalized ray method, Small and Booker [18] solved a multi-layered system by the flexibility matrix method.

Recently the BIEM has been applied to many seismic wave propagation problems [19-21]. This is because the radiation condition due to energy dissipation is automatically satisfied and the discretization is performed only on the boundary of the body. Extensive information on the BIEM for dynamic problems can be found in review type works such as the paper of Beskos [22], Dominguez and Alarkon [23], Kobayashi [24] and the book by Manolis and Beskos [25].

Most of the works are devoted to the multi-layered regions with simple geometry of the boundary between layers (usually parallel boundaries) and concern pure elastic mechanical soil properties. To the authors opinion there is a lack of studies involving both multi-layered regions with complex geometry of the boundaries between layers and with accounting for the non-elastic soil behavior.

In this paper, the two-dimensional "in-plane" wave propagation problem in the multi-layered geological region, shown in Figure (4) is considered. The stress-strain state is a plane strain state. The GMG model, discussed above, describes the non-elastic soil media. The equations governing the two-dimensional motion of the non-elastic media are Eq. (15), where the wave vectors are different for the different layers.
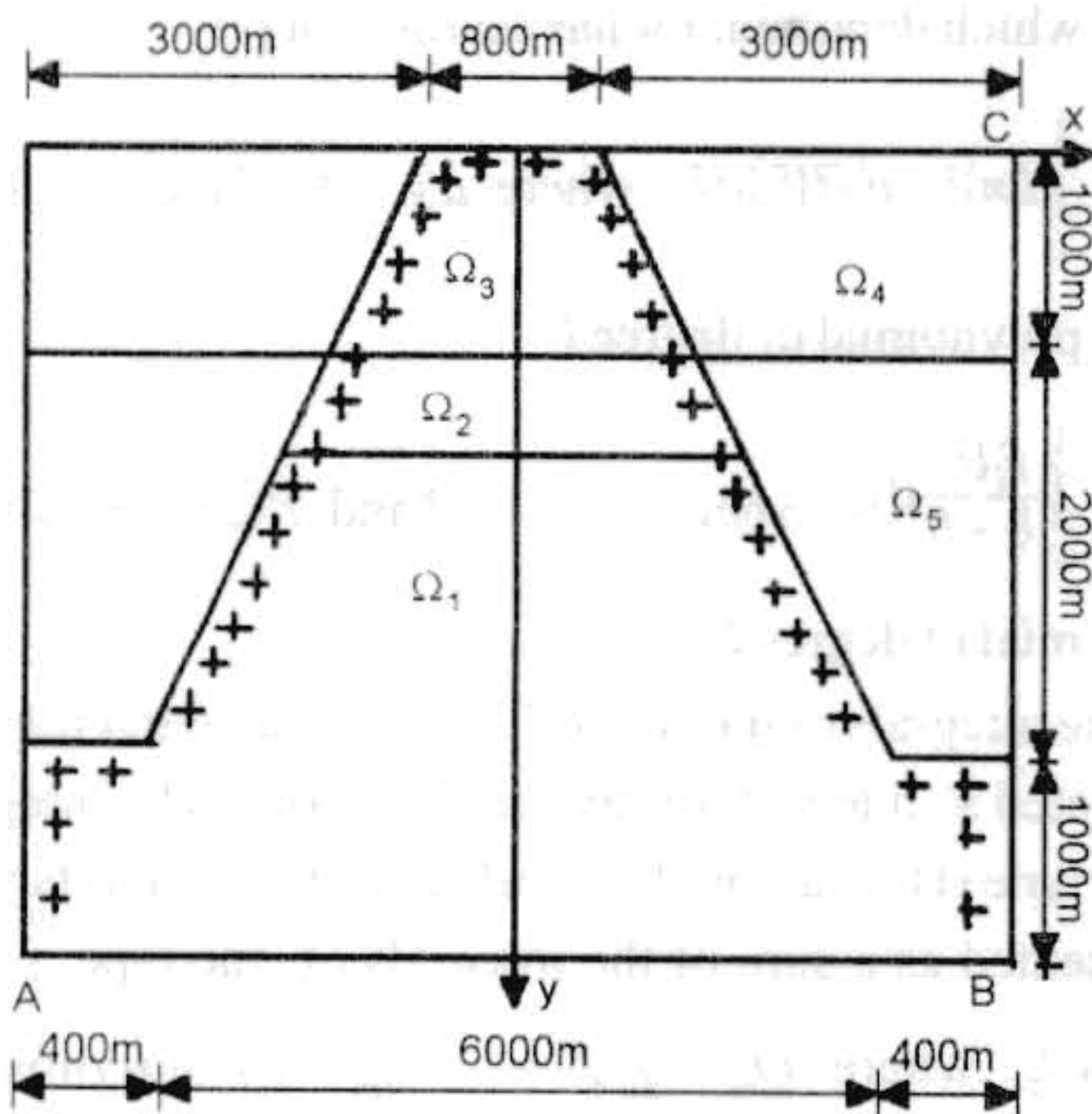

Figure 4. The geometry (2D) of the multi-layered geological region in 1951.

Due to the reason that the problem is axial-symmetric, it will be taken the half of the geometry. Two real geological situations for the multi-layered soil media with existence of salt ore deposits (see the half of the geometry in Figures (5) and (6)) are considered. These situations concern one and the same geological region but in

different periods of its exploitation - in 1951, see Figure (5) and 1994, see Figure (6). There is a change of the situation during the years when the exploitation of the salt ore deposits has been done. The main goal is to show that the changes in the soil region during all these years lead to the change in its dynamic response, i.e. to the change in the obtained theoretical seismograms.

The boundary conditions are, see Figures (5) and (6)

$$\sigma_{ij} \, n_j = 0 \text{ for } (x, y) \in FJ \text{ - free surface} \tag{17}$$

$$u_i^{(k)}(x, y) = u_i^{(k+1)}(x, y); \sigma_{ij}^{(k)} n_j^{(k)} = \sigma_{ij}^{(k+1)} n_j^{(k+1)} \text{ for } (x, y) \text{ on}$$
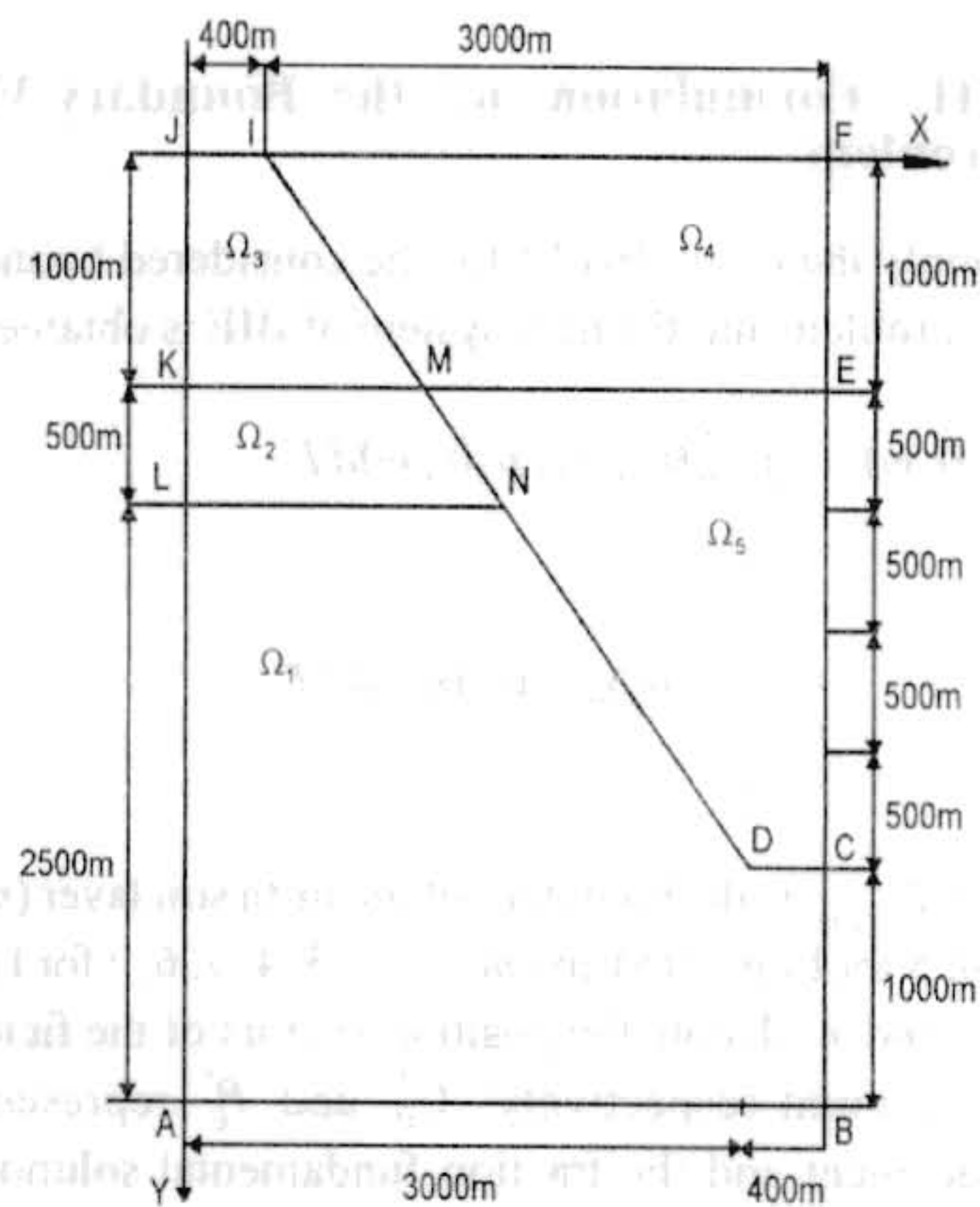the boundaries between the layers; k is the number of the layer Ω_k

Figure 5. A half of the geometry of the geological region in 1951.
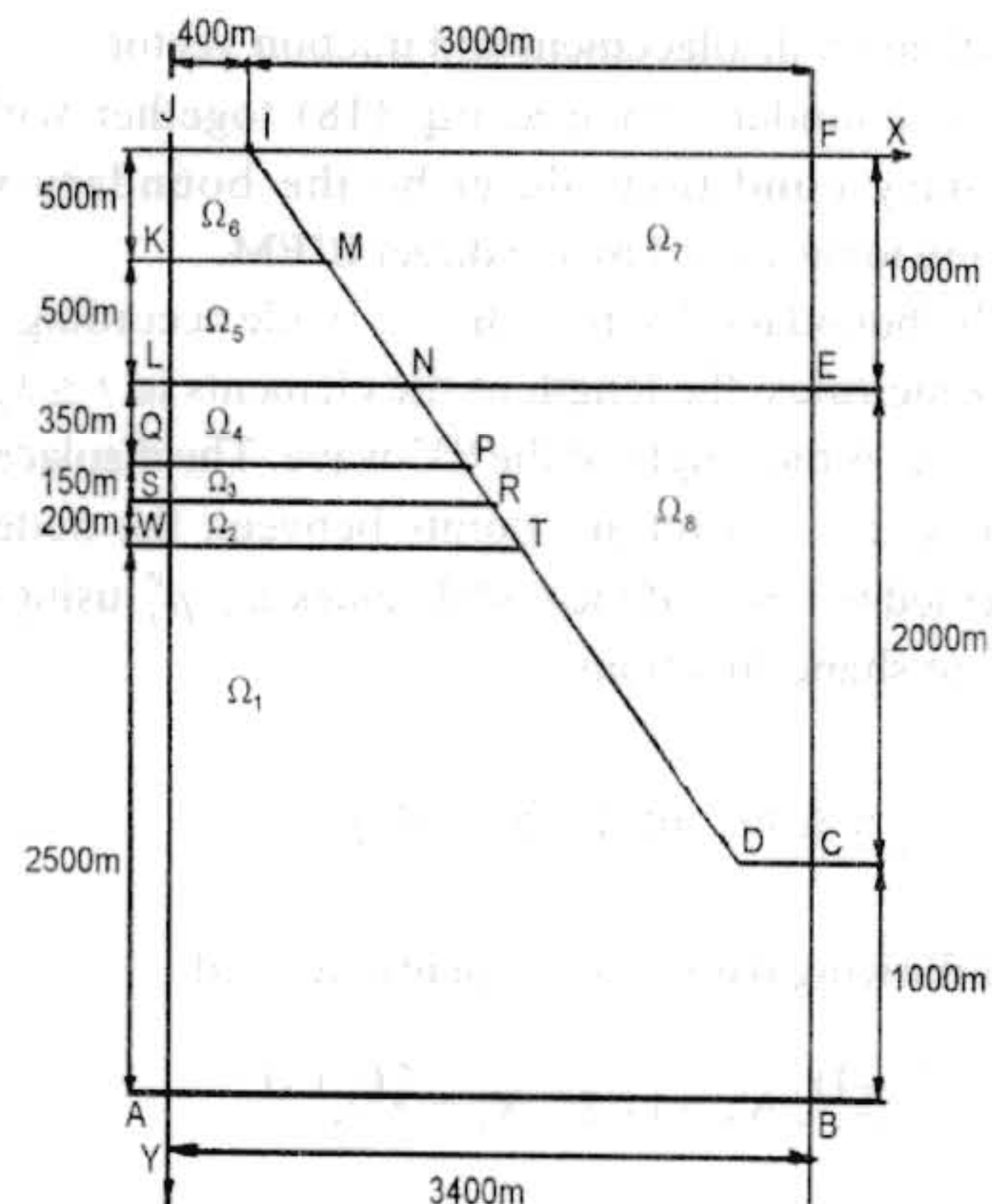

Figure 6. A half of the geometry of the geological region in 1994.

$P_y = \sigma_{yx} n_x + \sigma_{yy} n_y = 0$ and $u_x(x, y) = 0$ for $(x, y) \in JA$, $u_i^e(x, y) = u_i^0; \sigma_{ij}^e n_j = \sigma_{ij}^0 n_j$ for $(x, y) \in AB, BC, CE, EF$, where $e = \Omega_1, \Omega_4$ and Ω_5 for Figure (5) and $e = \Omega_1, \Omega_7$ and Ω_8 for Figure (6).

Here u_i^0, σ_{ij}^0 are the displacement and the traction, beyond the finite multi-layered region ABFJ, obtained by the sum of both: a) the waves scattered by the boundary ABFJ; b) the waves as a result of the interference between incident and reflected waves of the free boundary, see [11]; u_i^e, σ_{ij}^e are the displacement and the traction in Ω_1, Ω_4 and Ω_5 for Figure (5) and correspondingly in Ω_1, Ω_7 and Ω_8 for Figure (6).

So, the governing Eq. (15) and the boundary conditions Eq. (17) formulate the boundary-value problem for the amplitude of the scattered wave field.

5. BIE Formulation of the Boundary-Value Problem

We apply the direct BIEM for the considered boundary-value problem and the next system of BIE is obtained

$$c_{ij} u_j(r, \omega) = \int_{\Gamma_{\Omega m}} U_{ij}^*(r, r_0, \omega) p_j(r_0, \omega) d\Gamma$$

$$- \int_{\Gamma_{\Omega m}} P_{ij}^*(r, r_0, \omega) u_j(r_0, \omega) d\Gamma \qquad (18)$$

where $\Gamma_{\Omega m}$ is the boundary of the m-th soil layer ($m = 1$, 2, 3, 4, 5 for Figure (5) and $m = 1, 2, 3, 4, 5, 6, 7$ for Figure (6)); r and r_0 denote the position vectors of the field and running point respectively; U_{ij}^* and P_{ij}^* represent the displacement and the traction fundamental solutions of the system, see Appendix at the end of Part II in the next issue of JSEE; c_{ij} are constants and depend only on the shape of the boundary at the position vector r; u and p are unknown displacement and traction vectors.

The boundary integral Eq. (18) together with the boundary conditions describe the boundary-value problem to be solved by the direct BIEM.

The boundary discretization is made according to the following rules: the length of the elements is $\ell \le \lambda_s / 10$, where λ_s is the length of the SV-wave. The displacement and traction at arbitrary points between the nodes are expressed in terms of the nodal values u_j^e, p_j^e using finite element shape functions

$$u(\xi) = \sum_1^3 N_j(\xi) u_j^e, \; p(\xi) = \sum_1^3 N_j(\xi) p_j^e$$

The following parabolic elements are used

$$N_1 = \frac{\xi(\xi - 1)}{2}, N_2 = 1 - \xi^2, N_3 = \frac{\xi(\xi + 1)}{2}$$

An intrinsic co-ordinate ξ is designed for each triplet of nodal points, taking values -1, 0, +1 at the first, middle

and third nodes respectively. Let (x^p, y^p) be the field point; (x_1^q, y_1^q) and (x_3^q, y_3^q) are the first and third points of the corresponding BE and $r_{x,1} = x_1^q - x^p, r_{y,1} = y_1^q - y^p$, $r_{x,3} = x_3^q - x^p, r_{y,3} = y_3^q - y^p$. The required coordinates of the Gaussian quadrature are used for quadratic BE- $r_i(\xi) = r_{i,1} + \frac{\xi + 1}{2}(r_{i,3} - r_{i,1})$ with Jacobean $J = \frac{1}{2}$. There are the next types of integrals in the BIEs - $\int_{-1}^{1} P_{ij}^*(\xi) N_k(\xi) J d\xi$ and $\int_{-1}^{1} U_{ij}^*(\xi) N_k(\xi) J d\xi$. When the distance between the field point and the running point r is not zero, the integrals are solved by the Gauss 32- point quadrature scheme. According to the asymptotic behavior of the functions P_{ij}^*, U_{ij}^* (see Appendix), near $r = 0$ the integrals of the second type have no singularities but the integrals of the first type have singularities leading to CPV integrals. The kernels of the integrals of the first type have singularities like $O\left(\frac{1}{1 \pm \xi}\right)$ for $\xi \to \pm 1$, that leads to the CPV integrals, the kernels of the integrals of the second type have singularities like $O(ln(1 \pm \xi)$ for $\xi \to \pm 1$, which leads to non-singular integrals. The analytical treatment of the singular integrals concerns the next two cases with respect to the position of the field point

i) The field point coincides with the middle point of the BE.

Then the next integrals are used for the solution of the integrals of the first and second type

(f1.1) $\int_{-1}^{1} R(\xi) d\xi$, where $R(\xi)$ is a rational function of ξ, which denominator has no roots in $[-1, 1]$

(f1.2) $\int_{-1}^{1} Ln|\xi - a| P_l(\xi) d\xi$, where $a \in [-1, 1]$ and $P_l(\xi)$ is a polynomial of degree l

(f1.3) $\int_{-1}^{1} \frac{P_l(\xi)}{\xi - b} d\xi$, where $b \in [-1, 1]$ and $P_l(\xi)$ is a polynomial of degree l

The integrals of the type (f1.1) are regular and they are calculated as integrals of rational functions. The integrals of the type (f1.2) are with a weak singularity and they are represented as a sum of the integrals of the type $\int_0^a Ln\xi Q_m(\xi) d\xi$, where $Q_m = q_0 \xi^m + \ldots + q_m$ is a polynomial. Then it is clear that

$$\int_0^a Ln\xi Q_m(\xi) d\xi = \lim_{\varepsilon \to 0} \int_\varepsilon^a Ln\xi Q_m(\xi) d\xi = \sum_0^m \frac{q_j a^{j+1}}{j + 1}$$

$$\left(Ln \, a - \frac{1}{j+1}\right)$$

The integrals of the type (f1.3) are singular and lead to the sum of integrals of the type

(f1.1) and of integrals of the CPV type

$$\int_{-1}^{1}\frac{d\xi}{\xi-b}=\lim_{\varepsilon\to0}\int_{-1}^{b-\varepsilon}\frac{d\xi}{\xi-b}+\int_{b+\varepsilon}^{1}\frac{d\xi}{\xi-b}=Ln\frac{1-b}{1+b}$$

The solution of the integrals of the first type leads to the solution of the integrals of the types (f1.1) and (f1.3), while the integrals of the second type lead to the solution of the integrals of the types (f1.1) and (f1.2).

ii) The field point coincides with an odd nodal point. Then the next integrals are used for the solution of the integrals of both types

(f2.1) $\int_{-1}^{1}R(\xi)d\xi$, where $R(\xi)$ is a rational function of ξ, which denominator has no roots in $[-1, 1]$

(f2.2) $\int_{-1}^{1}Ln(\xi+1)P_l(\xi)d\xi$, $\int_{-1}^{1}Ln(1-\xi)P_l(\xi)d\xi$, where $P_l(x)$ is a polynomial of degree l

These two types integrals are solved as the integrals of the types (f1.1) and (f1.2)

(f2.3) $\int_{-1}^{1}\frac{P_l(\xi)}{1+\xi}d\xi$, $\int_{-1}^{1}\frac{Q_l(\xi)}{1-\xi}d\xi$, where $P_l(\xi), Q_l(\xi)$ are polynomials of degree l

$z_1^s = z_3^{s-1}$ is an odd nodal point used as a field point, $s, s-1$ are the numbers of the both neighboring BE. The odd points are used as allocation points for continuous shape function, so it is fulfilled $Q_l(1)=P_l(1)$. We change the variables and add the integrals over Γ^{s-1} and Γ^s, and the result is a CPV integral. Then the integral of the type (f2.3) can be expressed by the integrals of the type (f1.3)

$$\int_{-2}^{0}\frac{\hat{Q}_l(\eta)}{\eta}d\eta+\int_{0}^{2}\frac{\hat{P}_l(\eta)}{\eta}d\eta=\int_{-2}^{2}\frac{S(\eta)}{\eta}d\eta$$

where

$$S(\eta)=\begin{cases}\hat{Q}_l(\eta) & \eta\in[-2,0]\\\hat{P}_l(\eta) & \eta\in[0,2]\end{cases}$$

Note that the condition $Q_l(1)=P_l(-1)$ provides that $S(\eta)$ is continuous at the point 0.

(f2.4) $\int_{-1}^{1}\frac{\hat{P}_l(\xi)}{1+\xi}\chi_a(\xi)d\xi$, $\int_{-1}^{1}\frac{\hat{Q}_l(\xi)}{1-\xi}\chi_b(\xi)d\xi$

where

$$\chi_a(\xi)=\begin{cases}0 & \xi\in[-1,a]\\1 & \xi\in(a,1]\end{cases}\text{ for }-1<a<1$$

$$\chi_b(\xi)=\begin{cases}1 & \xi\in[-1,b]\\0 & \xi\in[b,1]\end{cases}\text{ for }-1<b<1$$

The integrals of the type (f2.4) are regular and they are sum of integrals of the type (f2.1). The solution of the integrals of the first type leads to the solution of integrals of the types (f2.1) and (f2.3), while the solution of the integrals of the second type leads to the solution of integrals of the types (f2.1) and (f2.2).

After the boundary discretization the system of integral equations is written at the discrete points, which are the nodal points of BE. An algebraic system according to the unknowns of the mixed boundary-value problem is obtained after the boundary condition satisfaction and solution of the singular and non-singular integrals.

6. Numerical Results

The physical properties of the geological region are given in Tables (1) and (2). The damping coefficients are $\alpha_s = 0.05$ for $\Omega_1, \Omega_2, \Omega_3$ and $\alpha_s = 0.001$ for the rest layers; $\alpha_p = 0.03$ for $\Omega_1, \Omega_2, \Omega_3$ and $\alpha_p = 0.005$ for the rest layers. The relaxation times for all layers are taken from [10]: $T_p = 0.2.10^{-8s}$ and $T_M = 100s$. The incidence wave angle according to axis Oy is 0^0. The geometrical parameters of the regions are given in Table (3). The theoretical seismograms of the horizontal $\frac{u_x}{u_0}$ and vertical $\frac{u_y}{u_0}$ displacements for soil column N1 at point (1000, 0.0) are shown in Figures (7) and (8) in both elastic and non-elastic cases. The theoretical seismograms of the horizontal $\frac{u_x}{u_0}$ and vertical $\frac{u_y}{u_0}$ displacements for soil column N2 at point (1000, 0.0) are shown correspondingly in Figures (9) and (10) in both elastic and non-elastic cases. Here u_0 is the amplitude of the incident wave. It is seen that the pure elastic case gives an unrealistic picture of the physical processes since when the frequency increases, the amplitude of the corresponding harmonics does not decrease. In the case of the Gurevich model the results are more realistic, since when the frequency increases the amplitudes of the corresponding harmonics damp, i.e. the real dynamic soil system acts as a low-frequency filter. One can see that in the case of the geological situation, shown in Figure (6), the amplitude-frequency characteristics are rather different from those for the geological situation, shown in Figure (5).

7. Conclusion

In this paper the theoretical seismograms obtained for a region with complex geometry and physics involve both kinds of seismic waves dispersion:

❖ Dispersion, due to the non-elastic soil behavior that is accounted for by the GMG model

❖ Dispersion, due to the wave geometrical scattering that is accounted for by the solution of the boundary-value problem by the direct boundary integral equation method.

The experimental results for the seismic wave

dispersion as well as the numerical results obtained for the seismic wave propagation on the base of the boundary integral equation method together with the GMG model prove the validity and advisability for the use of this model in seismic wave propagation problems. This model has in itself a possibility for connection and transition between the macro stress-strain processes and the microstructure state of the soil material. One can see that the change of the geological situation during the years when the exploitation of the salt ore deposits leads

Table 1. Physical constants of the geological column N1.

Number of Range	Material	Density $[kg/m^3]$	Lame Constant $[N/m^2]$	Poisson Constant	Shear Module $[N/m^2]$	Wave Shear Velocity $[m/s]$	Wave Long. Velocity $[m/s]$
Ω_1	Salt	$2,23.10^3$	$0,783.10^{10}$	0,33	$0,4026.10^1$	1343,6	2668,7
Ω_2	Salt	$2,23.10^3$	$0,8611.10^{10}$	0,33	$0,4425.10^1$	1408,6	2798
Ω_3	Salt	$2,2.10^3$	$0,9246.10^{10}$	0,35	$0,3974.10^1$	1344	2798
Ω_4	Surround rock	$2,2.10^3$	$0,75.10^{10}$	0,3	$0,5.10^{10}$	1507,55	2820,4
Ω_5	Surround rock	$2,6.10^3$	$0,2607.10^{11}$	0,3	$0,175.10^{11}$	2594,37	4847

Table 2. Physical constants of the geological column N2.

| Number of Range	Material	Density $[kg/m^3]$	Lame Constant $[N/m^2]$	Poisson Constant	Shear Module $[N/m^2]$	Wave Shear Velocity $[m/s]$	Wave Long. Velocity $[m/s]$
Ω_1	Salt	$2,23.10^3$	$0,7808.10^{10}$	0,33	$0,4026.10^{10}$	1343,64	2668,85
Ω_2	Salt	$2,21.10^3$	$0,76625.10^{10}$	0,33	$0,3945.10^{10}$	1336,06	2652,79
Ω_3	Salt	$2,23.10^3$	$0,86112.10^{10}$	0,33	$0,4425.10^{10}$	1408,65	2798,24
Ω_4	Salt	$2,20.10^3$	$0,8246.10^{10}$	0,33	$0,4248.10^{10}$	1389,57	2758,62
Ω_5	Salt	$1,68.10^3$	$0,4232.10^{10}$	0,33	$0,2186.10^{10}$	1140,69	2263,06
Ω_6	Salt	$2,2.10^3$	$0,9247.10^{10}$	0,33	$0,3974.10^{10}$	1344	2795,69
Ω_7	Surround Rock	$2,2.10^3$	$0,75.10^{10}$	0,3	$0,5.10^{10}$	1507,55	2820,4
Ω_8	Surround Rock	$2,6.10^3$	$0,2607.10^{11}$	0,3	$0,175.10^{11}$	2594,37	4847
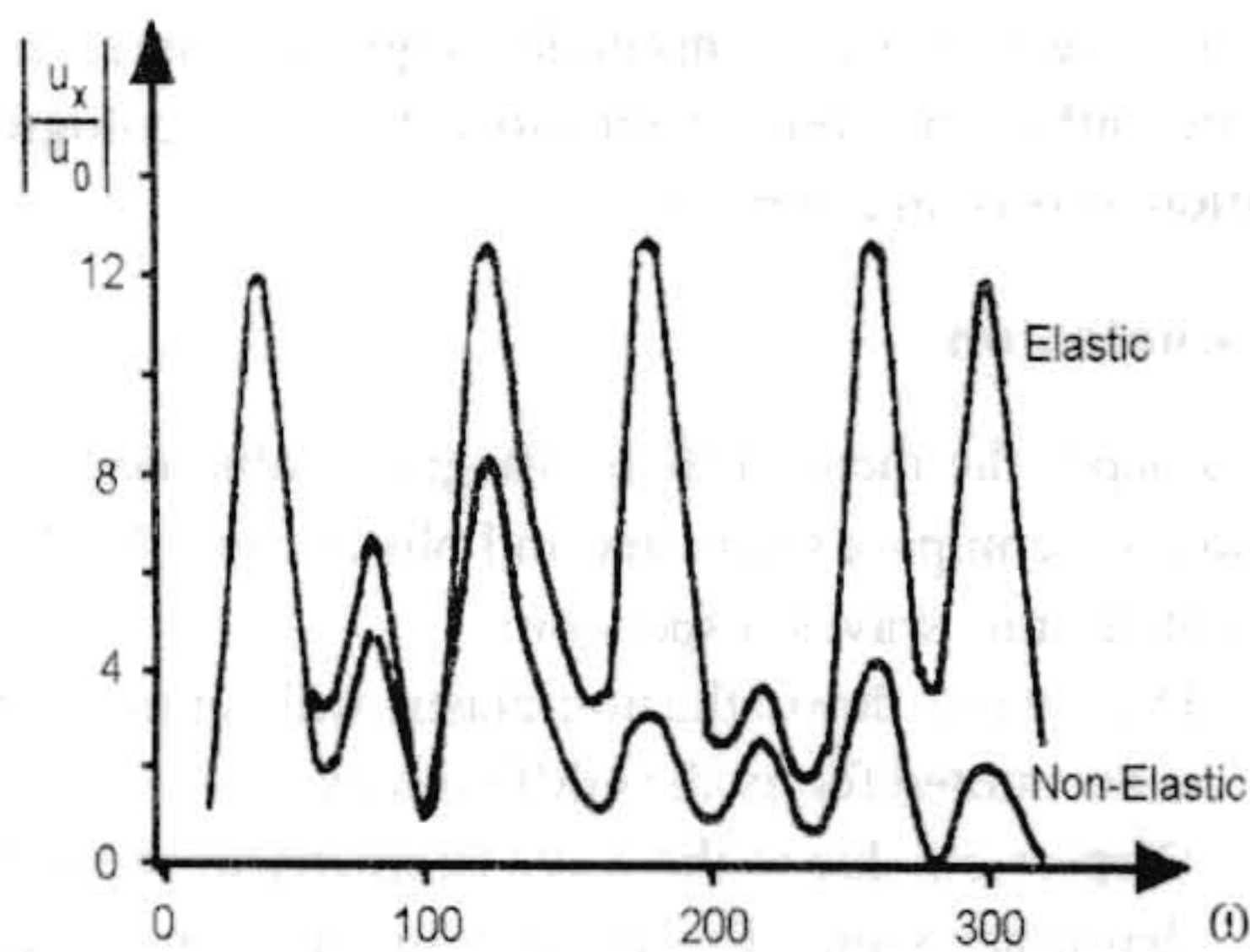
Figure 7. Amplitude-frequency characteristic of the horizontal component of the displacement $\frac{u_x}{u_0}$ for the region in Figure 5.
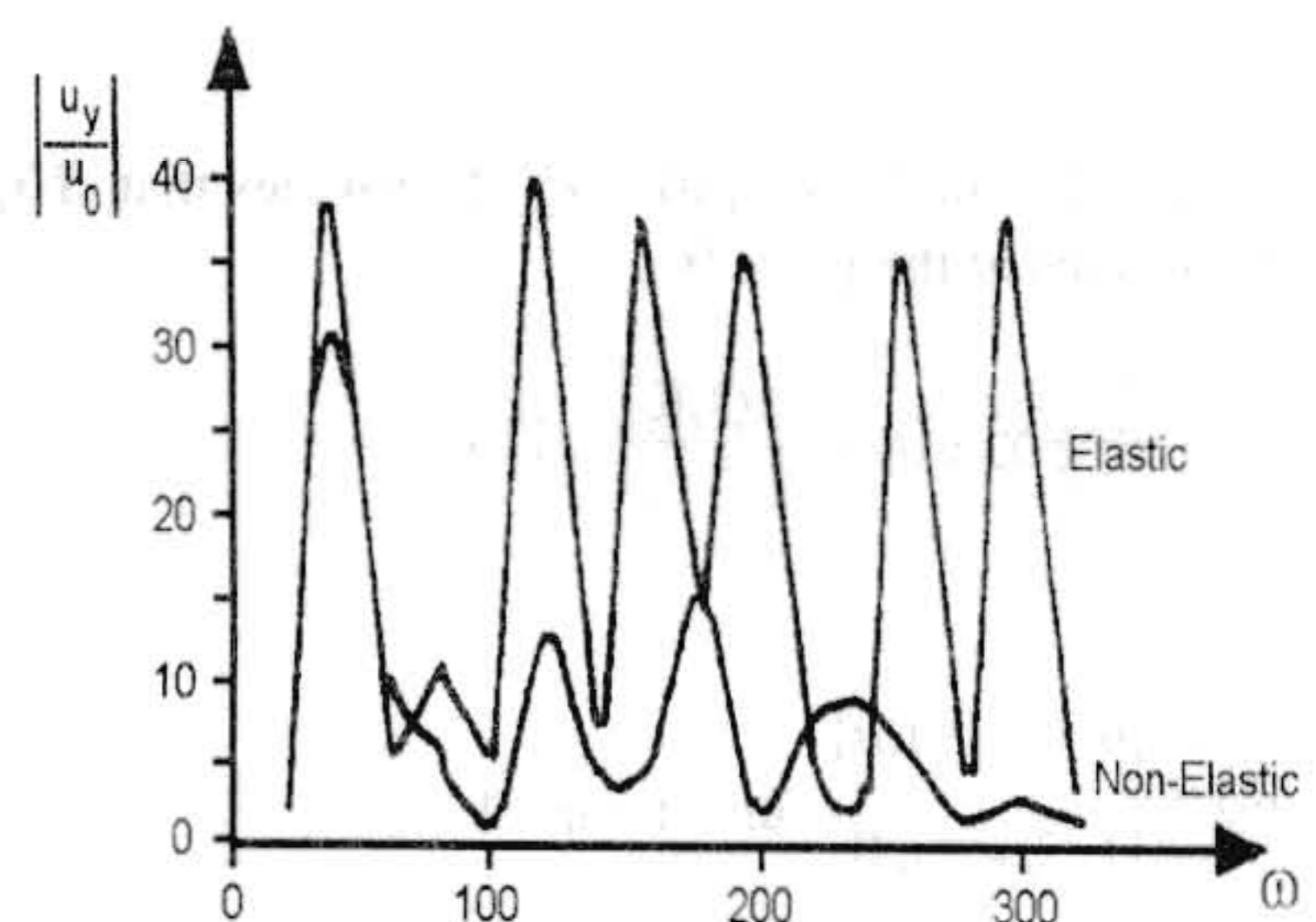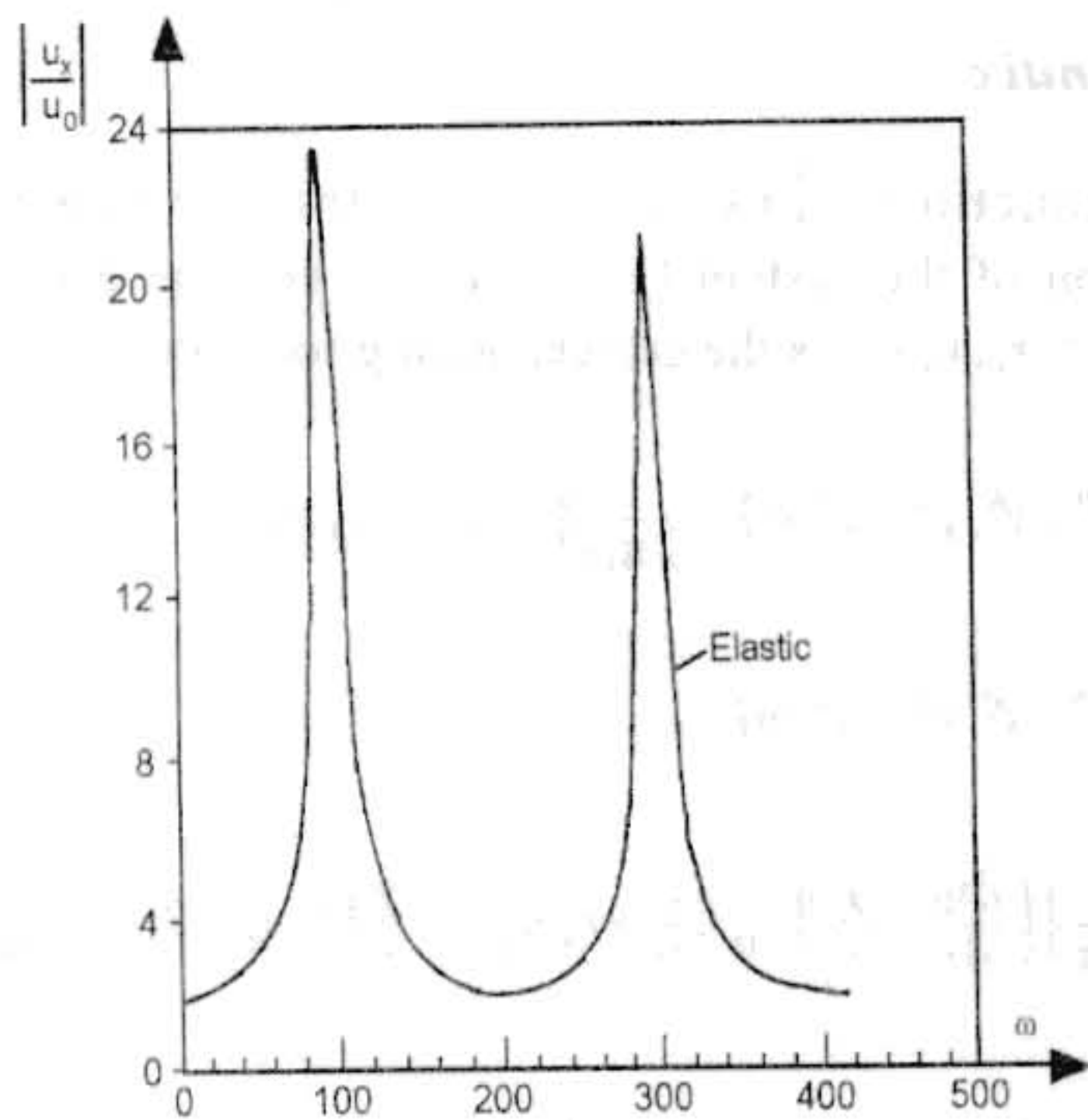

Figure 8. Amplitude-frequency characteristic of the vertical component of the displacement $\frac{u_y}{u_0}$ for the region in Figure 6 in the elastic case.

Table 3. Geological parameters of the geological column N1.

Boundary	Length
AB	3400
BC	1000
CE	2000
EF	1000
FI	3000
IJ	400
JK	1000
KL	500
LA	2500

Figure 10. Amplitude-frequency characteristic of the vertical component of the displacement $\frac{u_y}{u_0}$ for the region in Figure 6 in the elastic and non-elastic cases.

Figure 9a. Amplitude-frequency characteristic of the horizontal component of the displacement $\frac{u_x}{u_0}$ for the region in Figure 6 in the elastic case.
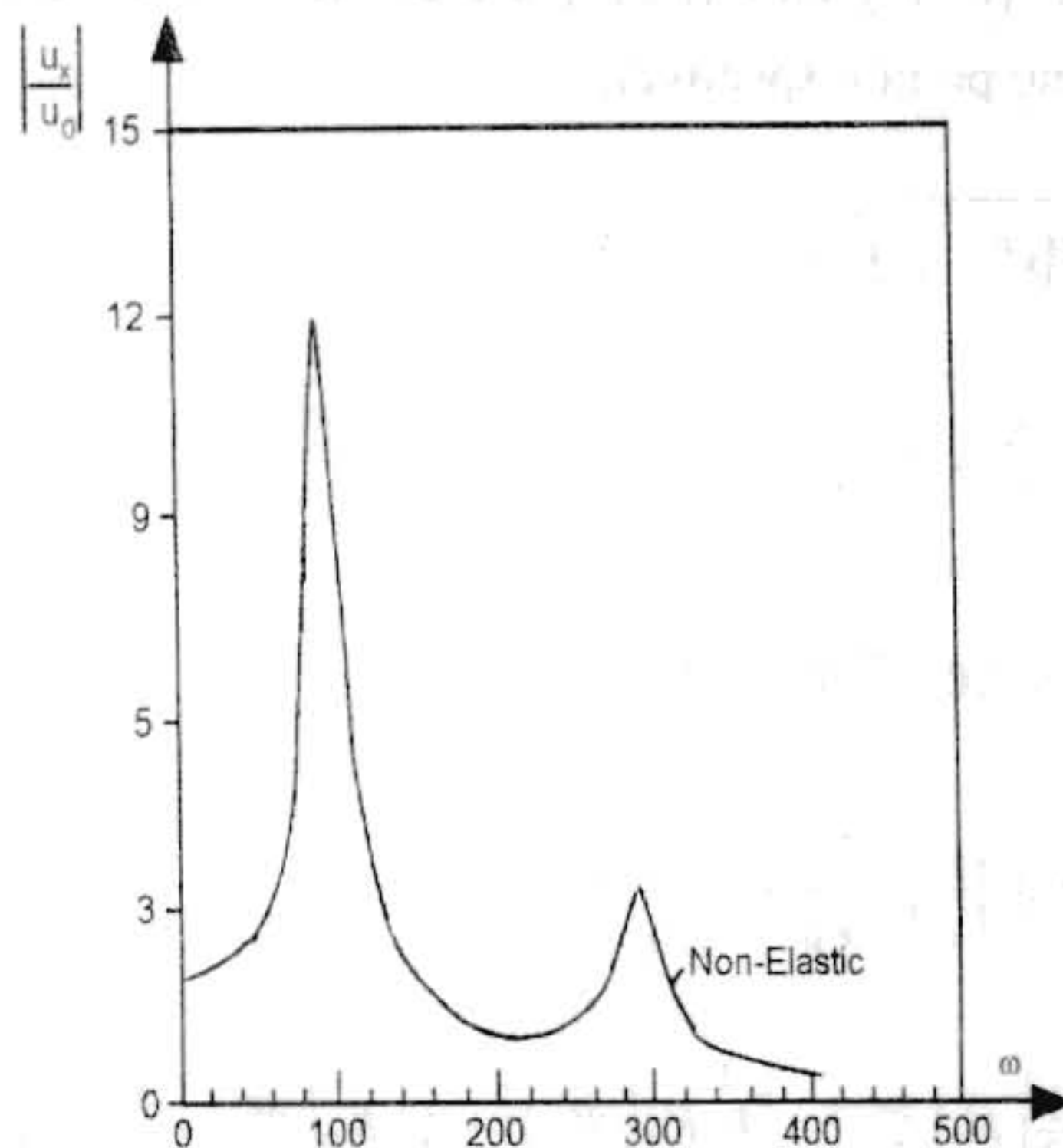

Figure 9b. Amplitude-frequency characteristic of the horizontal component of the displacement $\frac{u_x}{u_0}$ for the region in Figure 6 in the non-elastic case.
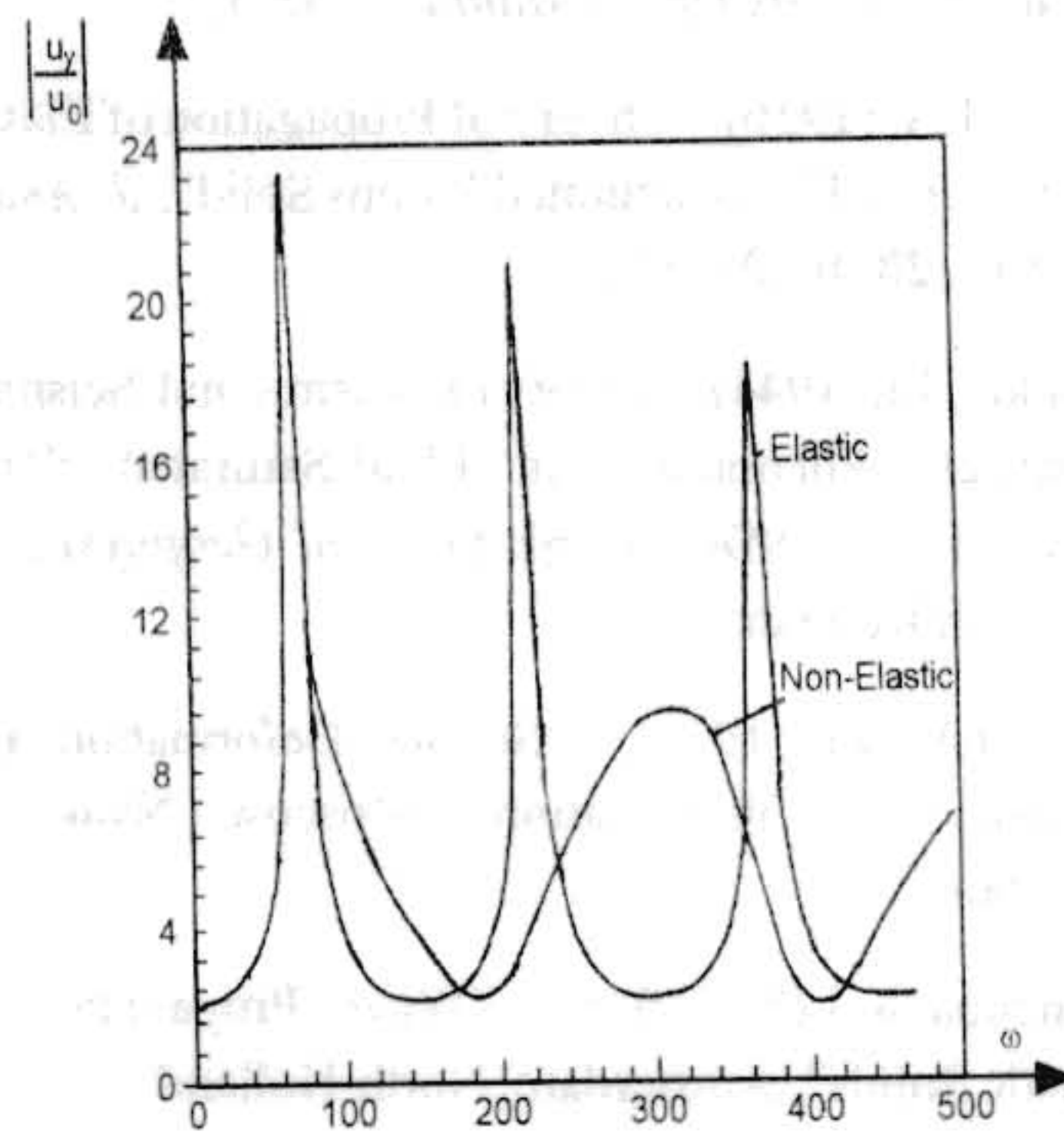
to the change of the time-harmonic wave picture. The amplitude-frequency characteristics of the surface responses are computed for real geological situations and different wave fields are obtained. These results show that the changes in the soil region lead to the change in its dynamic response, i.e. to the change in the obtained theoretical amplitude-frequency characteristics. All this assures us that the exploitation process leads to the changes in the geological situation of the region, and respectively to the changes of the soil response during eventual earthquake. Part of these results is reported on the Post-SMiRT 14 International Seminar, Pisa, Italy [12].

References

1. Kondratieva, T. (1971). "On Damping of Seismic Waves in Nonhomogeneity Field", *Izwestia USSR*, **4**, 56-86.

2. Deriagin, B. (1931). "About Damping and Dispersion of Seismic Waves", *J. of Geophysics*, **1**, 36-48.

3. Lomnitz, C. (1957). "Linear Dissipation in Solids", *J. Appl. Physics*, **28**, 18-26.

4. Futerman, W. (1962). "Dispersive Body Waves", *J. Geophysics Res.*, **67**(13), 73-84.

5. Knopoff, L. and Mac-Donald, G. (1958). "Attenuation of Small Amplitudes Stresses Waves in Solids", *Rev. Modern Phys.*, **30**, 63-72.

6. Isacovich, M.A. (1984). "On the Damping of Sound in Polycristals", *J. of Experimental and Theoretical Physics*, **18**, 64-75, in Russian.

7. Magnitski, W.A. and Jarkov, W.N. (1970). "The Nature of Layers with Reducing Seismic Wave Velocities in Upper Earthquake", *Proc. on Problems of Earth*

Structure and Its Upper Mantle, **7**, 38-42.

8. Biot, M.A. (1956). "Theory of Propagation of Elastic Waves in a Fluid-Saturated Porous Solid", *J. Amer. Ac. Soc.*, **28**, 1012-1020.

9. Frankel, J.I. (1944). "Theory of Seismic and Seismic-Electrical Phenomena in Fluid-Saturated Soil", *Izwestia An USSR, Geography and Geophysics*, **4**, 62-82, in Russian.

10. Gurevich, G.I. (1974). "Solides Deformation and Seismic Wave Propagation", Moscow, Nauka, in Russian.

11. Achenbach, J.D. (1975). "Wave Propagation in Elastic Solids", Amsterdam, North-Holland.

12. Dineva, P. and Gavrilova, E. (1997). "Generalized Maxwell-Gurevich Model for Seismic Wave Propagation Problems", *Proc. of the Post-SMiRT 14 Int. Seminar*, Pisa, Italy, 28-33.

13. Thompson, W.T. (1950). "Transmission of Elastic Waves through a Stratified Solid Medium", *J. of Applied Physics*, **21**, 89-93.

14. Haskell, N.A. (1953). "The Dispersion of Surface Waves on a Multilayered Media", Bulletin of the Seismological Society of America, **43**, 17-34.

15. Gilbert, F. and Backus, G.E. (1966). "Propagator Matrices in Elastic Wave and Vibration Problems", *Geophysics*, **31**, 326-332.

16. Fuchs, K. and Muller, G. (1971). "Computation of Synthetic Seismograms with the Reflectivity Method and Comparison of Observations", *Geophysical J. of the Royal Astronomical Society*, **23**, 417-433.

17. Pao, Y.H. and Gajewski, R.R. (1977). "The Generalized Ray Theory and Transient Responses of Layered Elastic Solids", *Physical Acoustics*, **13**, Academic Press, New York, 183-265.

18. Small, J.C. and Booker, J.R. (1986). "Finite Layer Analysis of Layered Elastic Materials Using Flexibility Approach", *Int. J. for Numer. Methods in Engr.*, **23**, 959-978.

19. Niwa, Y., Fukui, T., Kato, S., and Fujiki, K. (1980). "An Application of the Integral Equation Method to Two-Dimensional Elastodynamics", *Theoretical and Applied Mechanics*, **28**, 281-290. Univ. of Tokyo Press.

20. Banerjee, P.K., Ahmad, S., and Manolis, G.D. (1986). "Transient Elastodynamic Analysis of Three-Dimensional Problems by BEM", *Earthquake Engr. Struct. Dyn.*, **14**, 933.

21. Brebbia, C.A. and Dominguez, J. (1992). "Boundary Elements: An Introductory Course", *Second Edition Comput. Mech. Publ. and McGraw-Hill Book*, Comp., Southampton and New York.

22. Beskos, D.E. (1987). "Boundary Element Methods in Dynamic Analysis", *Appl. Mech. Reviews*, **40**, 1-23.

23. Dominguez, J. and Alarkon, E. (1981). "Elastodynamics, In Progress in BEM", **1**, *C.A. Brebbia (Ed.)*, 213-257, Pentech Press, London.

24. Kobayashi, S. (1987). "Elastodynamics, In BEM in Mechanics", *D.E. Beskos (Ed.)*, 191-255, North-Holland, Amsterdam.

25. Manolis, G.D. and Beskos, D.E. (1988). BEM in Elastodynamics, Unwin Hyman, London.

Appendix

The function $U_{kj}^*(x,y,x_0,y_0,\omega)$ is the fundamental solution of the system (15) in Part I and the function $P_{kj}^*(x,y,x_0,y_0,\omega)$ is the corresponding traction

$$U_{kj}^*\left(x^p - x^q, y^p - y^q, \omega\right) = \frac{1}{2\pi\mu}\left[\psi\delta_{kj} - \chi r_{,k} r_{,j}\right]$$

$$P_{kj}^*\left(x^p - x^q, y^p - y^q, \omega\right) =$$

$$\frac{1}{2\pi}\left\{\left(\frac{\partial\psi}{\partial r} - \frac{\chi}{r}\right)\left(\delta_{kj}\frac{\partial r}{\partial n} + r_{,k} n_j\right) - 2\frac{\chi}{r}\left(r_{,j} n_k - 2 r_{,k} r_{,j}\frac{\partial r}{\partial n}\right)\right\}$$

$$-\frac{1}{2\pi}\left\{2\frac{\partial\chi}{\partial r} r_{,k} r_{,j}\frac{\partial r}{\partial n} - \left(\frac{V_P^2}{V_S^2} - 2\right)\left(\frac{\partial\psi}{\partial r} - \frac{\partial\chi}{\partial r} - \frac{\chi}{r}\right) r_{,j} n_k\right\}$$

where $\left(x^p, y^p\right)$ and $\left(x^q, y^q\right)$ are the field point and the running point respectively

$$r = \sqrt{\left(x^p - x^q\right)^2 + \left(y^p - y^q\right)^2}$$

$$r_{,x}q = \frac{r_x}{r} = \frac{x^q - x^p}{r}, r_{,y}q = \frac{r_y}{r} = \frac{y^q - y^p}{r}$$

$$\frac{\partial r}{\partial n} r_{,x}q\, n_{,x}0 + r_{,y}q\, n_{,y}0, s = -i\omega$$

$$\chi = K_2\left(\frac{sr}{V_s}\right) - \frac{V_s^2}{V_P^2} K_2\left(\frac{sr}{V_p}\right)$$

$$\psi = \frac{1}{2}\left[K_2\left(\frac{sr}{V_s}\right) - \frac{V_s^2}{V_P^2} K_2\left(\frac{sr}{V_p}\right)\right] + \frac{1}{2}\left[K_0\left(\frac{sr}{V_s}\right) + \frac{V_s^2}{V_P^2} K_0\left(\frac{sr}{V_p}\right)\right]$$

The function $K_m(z) = -\frac{1}{2}i\pi(i)^m H_m^{(2)}(iz)$ for $z = -\frac{i\omega}{V_s}$ or

$z = -\dfrac{i\omega}{V_p}$ is represented with the modified Bessel functions of second type.

The asymptotic representations of the functions U_{kj}^* and P_{kj}^* for $r \to 0$ are

$$\left(U_{kj}^*\right)^{as} \approx$$

$$-\frac{1}{4\pi\mu}\left\{\left[\left(1+\frac{V_S^2}{V_P^2}\right)lnr + ln\frac{\omega}{2V_S} + \frac{V_S^2}{V_P^2}ln\frac{\omega}{2V_P}\right]\delta_{kj} - A\right\}$$

$$\left(P_{kj}^*\right)^{as} \approx -\frac{1}{2\pi r}\frac{V_S^2}{V_P^2}\left\{\left[\delta_{kj} + 2\left(1+\frac{V_S^2}{V_P^2}\right)r_{,k}r_{,j}\right]\frac{\partial r}{\partial n} - BB\right\}$$

where

$$A = -\frac{1}{4\pi\mu}\left\{\left(1-\frac{V_S^2}{V_P^2}\right)r_{,k}r_{,j} + i\frac{3\pi}{2}\left(1+\frac{V_S^2}{V_P^2}\right)\right\}$$

and

$$BB = -\frac{1}{2\pi r}\frac{V_S^2}{V_P^2}\left[n_k r_{,j} - n_j r_{,k}\right].$$